Journal of Solid State Chemistry 182 (2009) 2725–2732

Contents lists available at ScienceDirect

Journal of Solid State Chemistry

journal homepage: www.elsevier.com/locate/jssc

Hexaferrites and phase relations in the iron-rich part of the system Sr–La–Co–Fe–O

N. Langhof *, M. Göbbels

Applied Mineralogy, GeoZentrum Nordbayern, University of Erlangen-Nuremberg, Schlossgarten 5a, 91054 Erlangen, Germany

ARTICLE INFO

Article history:
Received 13 May 2009
Received in revised form
30 June 2009
Accepted 4 July 2009
Available online 21 July 2009

Keywords:
Hexagonal ferrites
La–Co substitution
M-type
Solid solution
$SrFe_{12}O_{19}$

ABSTRACT

The iron rich part of the system was examined in the temperature range of 1200–1380 °C in air, with focus on the solid solutions of M-type hexaferrites. Samples of suitable compositions were studied by electronprobe microanalysis (EPMA). Substituted Sr-hexaferrites in the system Sr–La–Co–Fe–O do not follow the 1:1 substitution mechanism of La/Co in M-type ferrites. Due to the presence and limited Co^{2+}-incorporation Fe^{3+}-ions are reduced to Fe^{2+} within the crystal lattice to obtain charge balance. In all examined M-type ferrites divalent iron is formed, even at 1200 °C. The substitution principle $Sr^{2+}+Fe^{3+} \leftrightarrow La^{3+}+(Fe^{2+}, Co^{2+})$ yields to the general substitution formula for the M-type hexaferrite $Sr^{2+}{}_{1-x}La^{3+}{}_{x}Fe^{2+}{}_{x-y}Co^{2+}{}_{y}Fe^{3+}{}_{12-x}O^{19}$ ($0 \le x \le 1$ and $0 \le y \le x$). In addition Sr/La-perovskite$_{SS}$ ($_{SS}$ = solid solution), Co/Fe-spinel$_{SS}$, hematite and magnetite are formed. Sr-hexaferrite exhibits at 1200 °C a limited solid solution with small amounts of Fe^{2+} ($SrFe_{12}O_{19} \leftrightarrow Sr_{0.3}La_{0.7}Co_{0.5}Fe^{2+}_{0.2}Fe_{11.3}O_{19}$). At 1300 and 1380 °C a continuous solid solution series of the M-type hexaferrite is stable. $SrFe_{12}O_{19}$ and $LaCo_{0.4}Fe^{2+}_{0.6}Fe_{11}O_{19}$ are the end members at 1300 °C. The maximum $Fe^{2+}O$ content is about 13 mol% in the M-type ferrite at 1380 °C ($LaCo_{0.1}Fe^{2+}_{0.9}Fe_{11}O_{19}$).

1. Introduction

Ba- and Sr-hexaferrites are the most important ceramic permanent magnets [1]. $BaFe_{12}O_{19}$ and $SrFe_{12}O_{19}$ are hexagonal compounds with elongated crystals along *c*-axis. The high magnetic coercive force, saturation magnetization and remanence enable different applications such as in the generation of microwaves, memories and high frequency electromagnetic devices. For example the saturation magnetization M_S of Sr-Hexaferrite at room temperature is about 74.3 A m^2/kg (emu/g) and the remanence B_R between 400 and 420 mT (4000 and 4200 Gs~Oe) [2,3]. Besides that the ferrites are economically favourable for production and have an excellent chemical stability [4,5]. Nevertheless it is necessary to improve the magnetic properties of those materials. Remanence is mainly influenced by the chemical composition and subsequently the position of iron or substituted ions in the magnetic sublattices. Co-substitution of Fe^{3+} and Sr^{2+} by other ions is a good approach to reach this aim. Moreover the grain size and shape are very important for anisotropy field and the coercive force. Coupled substitution by La^{3+} and Co^{2+} gives the possibility to enhance the magnetic properties of M-type ferrites. Magnets with remanence B_r = 440–450 mT (4400–4500 Gs~Oe) and coercivity H_{ci} = 360–380 kA/m were produced [6–11].

Aim of this study is to examine the phase relations in the iron rich part of the system Sr–La–Co–Fe–O. First investigations at 1300 °C in this system lead to the conclusion that Fe^{2+} is already formed at temperatures of 1300 °C in air. Therefore the substitution formula $Sr^{2+}{}_{1-x}La^{3+}{}_{x}Fe^{2+}{}_{x-y}Co^{2+}{}_{y}Fe^{3+}{}_{12-x}O^{19}$ ($0 \le x \le 1$ and $0 \le y \le x$) was determined by [6,12]. Other authors consider the formation of divalent iron without describing the influence of this ion on the magnetic properties. This leads to the substitution formula $Sr_{1-x}La_xCo_xFe_{12-x}O_{19}$ ($0 \le x \le 1$) [13–16]. This study is focussed on the presence of Fe^{2+}-ions in the M-type hexaferrites, the existence and the extent of solid solutions at different temperatures (1200, 1300 and 1380 °C).

2. Experimental

To determine the phase relations suitable samples were prepared by mixing Fe_2O_3 (Riedel-de Haën, >97%), $SrCO_3$ (Aldrich, >98%), La_2O_3 (Alfa Aesar, >99.99%) and $CoCO_3$ (Alfa Aesar, >99%). Chosen mixtures were homogenized, milled with a vibratory disc mill RETSCH RS 1 (grinding tool:hardened steel) and decalcinated for 20 h at 1000 °C in air. Subsequently samples were cold isostatic pressed into tablets of about 1 cm in diameter. Afterwards small samples (about 0.5 cm^3) were synthesized in platinum containers at 1200, 1300 and 1380 °C. Because of the

* Corresponding author. Fax: +49 9131 8523734.
E-mail address: langhof@geol.uni-erlangen.de (N. Langhof).

0022-4596/$ - see front matter © 2009 Elsevier Inc. All rights reserved.
doi:10.1016/j.jssc.2009.07.024

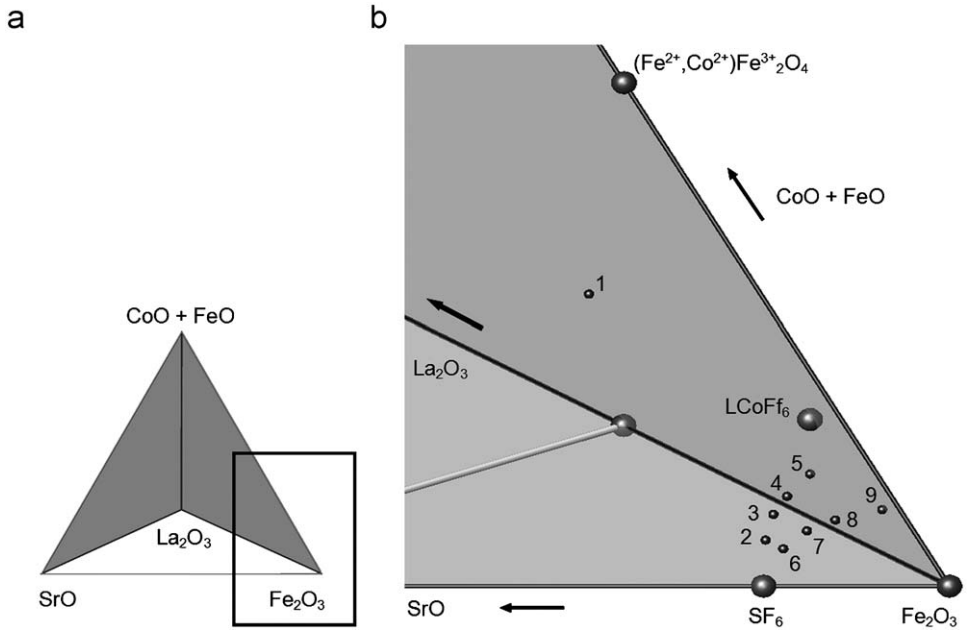

Fig. 1. (a) Phase diagram of the system Sr–La–Co–Fe–O (investigation area is marked with square). (b) Chosen mixtures 1–9; $SF_6 = SrFe_{12}O_{19}$; $LCoFf_6 = LaFe^{2+}_{1-y}Co_yFe^{3+}_{11}O_{19}$ ($0.5 \geq y \geq 0.2$); LF–P = $LaFeO_3$ (La–Fe perovskite).

stability range of La-hexaferrite between 1360 and 1410 °C [17] 1380 °C was chosen. All experiments were sintered in vertical tube furnaces in air. Temperatures were controlled by a $Pt_{94}Rh_6$–$Pt_{70}Rh_{30}$ thermocouple, calibrated according to the IPTS-68 temperature scale on the melting point of gold (1064.4 °C). The reported temperatures of this investigation are assumed to be correct within ±5 °C. Suitable sintering times were chosen to get grain sizes of minimum 10 μm in diameter to obtain good microprobe analysis. Synthesis times in the range of 1 day up to 30 days were chosen. After quenching in water, samples were embedded in epoxy resin, polished and coated with carbon. To identify the phase relations and to determine the chemical composition an electronprobe microanalysis (EPMA: JEOL JXA-8200) was used. Areas of about 150 μm^2 were accomplished to determine phase relations in thermodynamic equilibrium conditions. The following parameters for these analyses were applied: beam current = 15 nA; acceleration voltage = 15 kV. Furthermore the measuring time per peak was 20 s (underground 10 s). Analysator crystals PET (pentaerythritol), TAP (thallium acid phthalate) and LIF (lithium fluoride) were used. The net intensities of characteristic X-ray lines were compared with those of the standard materials celestine ($SrSO_4$), hematite (Fe_2O_3), Co (metal) and $LaPO_4$ (lanthanum phosphate). To obtain the composition of different phases the ZAF correction method was applied. At least five measuring points for each phase were determined. An absolute error for the EPMA measurement is assumed to be <1%. In some cases the phase relations were confirmed additionally by X-ray powder diffraction (Siemens D-5000, Cu$K\alpha_1$ = 1.54056 Å, 40 kV, 30 mA, 2θ: 5–80°, step: 0.02°, dwell time: 4 s). The FeO content was always calculated by mineral formula calculation [18] and proved by chemical titration [19]. At first the single phase powdered samples were dissoluted in hydrochloric acid in argon. Subsequently the Fe^{2+} was titrated with a 0.05 N Ce^{4+} solution under a flow of argon with potentiometric detection of the equivalent point. The detection limit of that titration is given by the first drop of Ce^{4+} solution ($V \approx 0.03$ ml), which corresponds to 0.08 wt% Fe^{2+} for 100 mg of a ferrite sample. Finally the compositions of the coexisting phases were plotted in several phase diagrams.

Table 1
Chemical composition of the mixtures in the system Sr–La–Co–Fe–O.

Chemical composition in mol%				
Sr–La–Co–Fe–O mixtures	SrO	CoO	La_2O_3	Fe_2O_3
1	8.93	25.00	12.50	53.57
2	10.60	3.43	3.61	82.36
3	7.62	4.95	6.85	80.58
4	4.64	5.79	9.87	79.70
5	0.10	6.43	14.78	78.69
6	10.60	3.43	0.90	85.07
7	7.62	4.95	1.71	85.72
8	4.64	5.79	2.47	87.10
9	0.10	6.43	3.70	89.77

3. Results and discussion

In this study samples were equilibrated at 1200, 1300 and 1380 °C. All samples are multi-phase. The complete subsolidus phase relations in the Fe-rich part of all systems were examined. Due to recrystallization chemical analyses of the melts were not suitable. Therefore their compositions were not measured. The microprobe analyses and the phase relations are presented in quaternary systems (Fig. 1). In order to display a quinary system in three-dimensions FeO and CoO were plotted together on one axis. The main aim is to determine the stability of the M-type ferrites and the extensions of possible solid solutions. To determine the phase relations nine mixtures were chosen at both sides of the presumed solid solution series (Fig. 1b). Mixtures 6–9 contain a significantly higher amount of Fe_2O_3 (Table 1). The expected substitution principle $Sr^{2+}+Fe^{3+} \leftrightarrow La^{3+}+(Fe^{2+}, Co^{2+})$ was confirmed at all chosen temperatures.

3.1. Hexaferrites and phase relations at 1200 °C

After sintering, the M-type hexaferrites were determined in several samples (Table 2). In addition to the microprobe

Table 2
M-type hexaferrites at 1200 °C in the system Sr–La–Co–Fe–O.

M-type hexaferrites at 1200 °C								
Mixtures	SrO (mol%)	La_2O_3 (mol%)	CoO (mol%)	FeO (mol%)	Fe_2O_3 (mol%)	La^{3+}	Co^{2+}	Fe^{2+}
						x	y	$x-y$
6	11.4	1.5	3.1	0.0	84.3	0.19	0.21	0.00
2	10.6	1.8	3.4	0.3	83.9	0.24	0.23	0.03
7	9.4	2.5	4.2	0.7	83.3	0.34	0.30	0.04
3	9.0	2.6	4.3	1.0	83.1	0.38	0.30	0.08
8	5.2	4.5	6.6	2.5	81.2	0.65	0.47	0.19
4	4.5	4.9	6.6	3.2	80.8	0.70	0.45	0.24
1	*10.0*	*1.6*	*6.0*	n.c.	*82.3*	–	–	–

M-type solid solution series: $Sr_{1-x}La_xFe^{2+}{}_{x-y}Co^{2+}{}_yFe^{3+}{}_{12-x}O^{19}$ ($0 \le x \le 0.7$ and $0 \le y \le 0.45$); mixture 1 = M-type hexaferrite with another substitution mechanism; n.c. = not calculated.

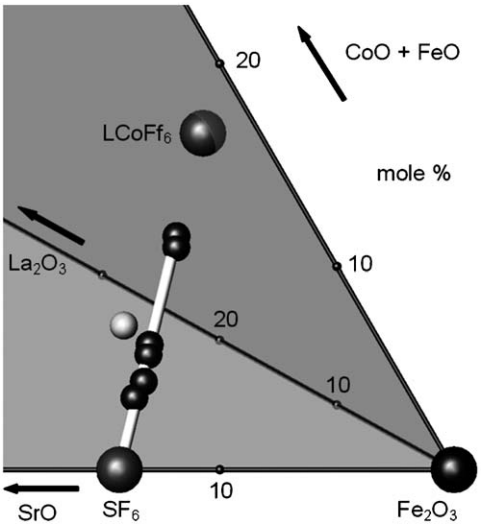

Fig. 2. M-type solid solution series $Sr_{1-x}La_xFe^{2+}{}_{x-y}Co^{2+}{}_yFe^{3+}{}_{12-x}O^{19}$ ($0 \le x \le 0.7$ and $0 \le y \le 0.45$) at 1200 °C; dark grey = data from electronprobe microanalyses; light grey = hexaphase formed in mixture 1; $SF_6 = SrFe^{3+}_{12}O_{19}$; $LCoFf_6$ = at 1200 °C hypothetic $LaFe^{2+}_{1-y}Co_yFe^{3+}_{11}O_{19}$ ($0 \le x \le 0.7$ and $0 \le y \le 0.45$); S = SrO; L = La_2O_3; Co = CoO; F = Fe_2O_3; f = FeO.

measurements the phase relations of the samples were confirmed by X-ray powder diffraction. Up to 70% of the Sr^{2+}-ions were replaced by La^{3+} (Fig. 2; Table 2). The end members of the solid solution at 1200 °C are $SrFe_{12}O_{19}$ and $Sr^{2+}_{0.30}La^{3+}_{0.70}Co^{2+}_{0.47}Fe^{2+}_{0.24}Fe^{3+}_{11.30}O_{19}$. At low substitution amounts (up to ~25%) the charge balance is obtained by incorporation of Co^{2+}-ions exclusively. For higher substitution amounts additional Fe^{2+}-ions are formed. Thus the substitution formula at 1200 °C is

$$Sr_{1-x}La_xCo_y{}^{2+}Fe^{2+}{}_{x-y}Fe^{3+}{}_{12-x}O_{19}$$

$$La^{3+}: 0 \le x \le 0.70$$

$$Co^{2+}: 0 \le y \le 0.47 \text{ and } Fe^{2+}: 0 \le x-y \le 0.24$$

In mixture 1 it is remarkable that a M-type hexaferrite was formed which differs from the substitution mechanism mentioned above (Fig. 2; Tables 1 and 2). This phase shows significant higher CoO contents, more than required to compensate the

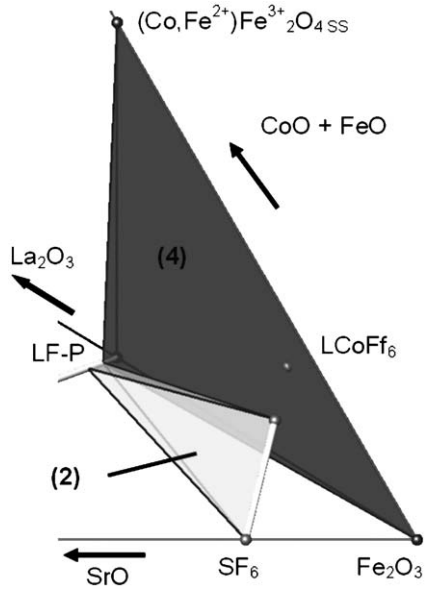

Fig. 3. Phase relations including phase polyhedra (2) perovskite$_{SS}$—M-type$_{SS}$ and (4) perovskite$_{SS}$—Co–Fe spinel$_{SS}$—hematite in the Fe-rich part of the system Sr–La–Co–Fe–O at 1200 °C (bold white lines = solid solution series); SF–P = Sr-perovskite $SrFeO_{3-\delta}$; SF–PD = Sr-perovskite-derivate $Sr_4Fe_6O_{13\pm\delta}$; LF–P = La-perovskite $LaFeO_3$; $LCoFf_6$ = at 1200 °C hypothetical M-type $LaFe^{2+}_{1-y}Co_yFe^{3+}_{11}O_{19}$; SF_6 = M-type Sr-hexaferrite $SrFe^{3+}_{12}O_{19}$; $(Co,Fe^{2+})Fe^{3+}_2O_{4\,SS}$ spinel solid solution; S = SrO; L = La_2O_3; Co = CoO; F = Fe_2O_3; f = FeO.

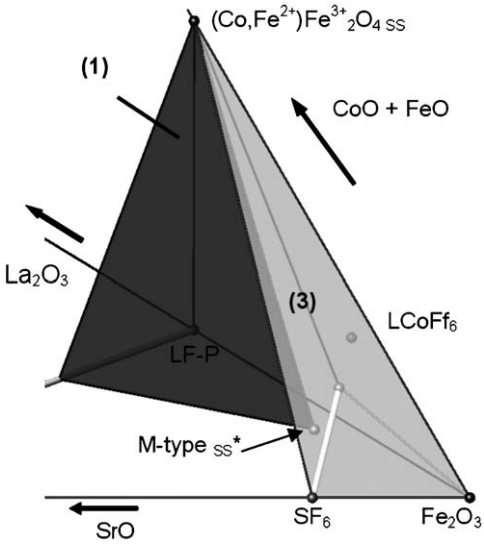

Fig. 4. Phase relations including phase polyhedra (1) perovskite$_{SS}$—M-type-$_{SS}$*—Co–Fe spinel$_{SS}$ and (3) M-type$_{SS}$—Co–Fe spinel$_{SS}$—hematite in the Fe-rich part of the system Sr–La–Co–Fe–O at 1200 °C (bold light grey lines = solid solution series); SF–P = Sr-perovskite $SrFeO_{3-\delta}$; SF–PD = Sr-perovskite-derivate $Sr_4Fe_6O_{13\pm\delta}$; LF–P = La-perovskite $LaFeO_3$; $LCoFf_6$ = at 1200 °C hypothetical M-type $LaFe^{2+}_{1-y}Co_yFe^{3+}_{11}O_{19}$; SF_6 = M-type Sr-hexaferrite $SrFe^{3+}_{12}O_{19}$; $(Co,Fe^{2+})Fe^{3+}_2O_{4\,SS}$ = spinel$_{SS}$; M-type $_{SS^*}$ = CoO-rich M-type solid solution formed by sintering of mixture 1; S = SrO; L = La_2O_3; Co = CoO; F = Fe_2O_3; f = FeO.

substitution of Sr^{2+} by La^{3+}. Probably this is an indication for two substitution mechanisms. The first above mentioned: $Sr^{2+}+Fe^{3+} \leftrightarrow La^{3+}+(Fe^{2+}, Co^{2+})$ and the second additional: 2 $Fe^{3+} \leftrightarrow (Fe^{2+}, Co^{2+})$. Therefore this phase is outside of the M-type solid solution series (Fig. 2). To check this theory further investigations are required. Nevertheless in mixtures 1–9 one can observe different coexisting phases (Figs. 3 and 4). Noticeable

Table 3
M-type hexaferrites at 1300 °C in the system Sr–La–Co–Fe–O.

M-type hexaferrites at 1300 °C								
Mixtures	SrO (mol%)	La_2O_3 (mol%)	CoO (mol%)	FeO (mol%)	Fe_2O_3 (mol%)	La^{3+} x	Co^{2+} y	Fe^{2+} $x-y$
6	11.7	1.2	1.9	0.7	84.5	0.17	0.13	0.05
2	10.9	1.8	3.0	0.5	83.9	0.25	0.21	0.04
7	9.1	2.5	2.8	2.3	83.2	0.35	0.20	0.16
3	7.6	3.4	4.7	2.0	82.3	0.47	0.33	0.14
8	6.8	3.6	3.5	4.0	82.1	0.51	0.25	0.28
4	4.9	4.8	5.2	4.2	80.9	0.68	0.37	0.29
9	0.3	6.8	5.8	8.2	78.9	0.95	0.41	0.57
5	0.3	7.3	5.8	8.2	78.5	1.00	0.40	0.57
*	–	7.1	5.3	9.1	78.5	1.00	0.37	0.63

M-type solid solution series: $Sr_{1-x}La_xFe^{2+}{}_{x-y}Co^{2+}{}_yFe^{3+}{}_{12-x}O^{19}$ ($0 \le x \le 1$ and $0 \le y \le 0.4$); * = La end member of the M-type$_{SS}$ observed in the La–Co–Fe–O system, derived from a forthcoming paper.

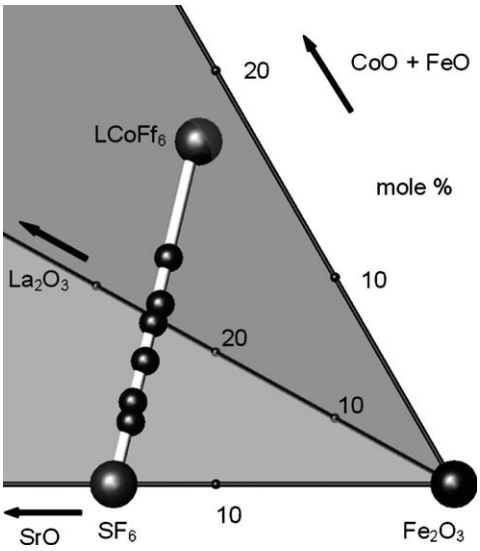

Fig. 5. M-type solid solution series $Sr_{1-x}La_xFe^{2+}{}_{x-y}Co^{2+}{}_yFe^{3+}{}_{12-x}O^{19}$ ($0 \le x \le 1$ and $0 \le y \le 0.4$) at 1300 °C; dark grey = data from electronprobe microanalyses; $SF_6 = SrFe^{3+}_{12}O_{19}$; $LCoFf_6 = LaCo_{0.4}Fe^{2+}_{0.6}Fe^{3+}_{11}O_{19}$; S = SrO; L = La_2O_3; Co = CoO; F = Fe_2O_3; f = FeO.

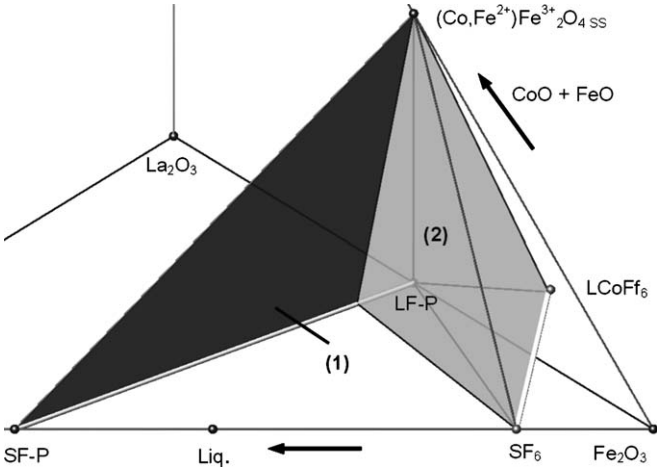

Fig. 6. Phase relations including phase polyhedra (1) perovskite$_{SS}$—Co–Fe spinel$_{SS}$ and (2) perovskite$_{SS}$—M-type$_{SS}$—Co–Fe spinel$_{SS}$ in the Fe-rich part of the system Sr–La–Co–Fe–O at 1300 °C (bold light grey lines = solid solution series); SF–P = Sr-perovskite $SrFeO_{3-\delta}$; LF–P = La-perovskite $LaFeO_3$; $LCoFf_6$ = M-type $LaFe^{2+}_{0.6}Co_{0.4}Fe^{3+}_{11}O_{19}$; SF_6 = M-type Sr-hexaferrite $SrFe^{3+}_{12}O_{19}$; $(Co,Fe^{2+})Fe^{3+}_2O_{4\,SS}$ = spinel$_{SS}$; S = SrO; L = La_2O_3; Co = CoO; F = Fe_2O_3; f = FeO.

are hematite and the solid solution series of perovskite $Sr_{1-x}La_xFeO_{3-\delta}$ ($0 \le \delta \le 0.5$ and $0 \le x \le 1$) and the spinel$_{SS}$ $Co_{1-x}Fe^{2+}{}_xFe^{3+}{}_2O_4$ ($0 \le x \le 0.45$). The perovskite$_{SS}$ contains about 1 mol% CoO, but it is negligible for the substitution formula. Furthermore, the calculated FeO content of spinel$_{SS}$ in the present work agrees with the phase diagram of Co–Fe–O in air [20].

3.2. Hexaferrites and phase relations at 1300 °C

The existing hexaferrites at 1300 °C are summarized in Table 3. There is a continuous solid solution series between pure Sr- and La-hexaferrite. All Sr^{2+}-ions were substituted by La^{3+}-ions and the charge balance is obtained by the incorporation of Fe^{2+}- and Co^{2+}-ions for Fe^{3+}. The composition of the Sr-free end member of the solid solution derived from a forthcoming paper about the system La–Co–Fe–O (signed with asterisks in Table 3). Fig. 5 shows the solid solution of M-type hexaferrites between the end members $SrFe_{12}O_{19}$ and $LaCo_{0.37}Fe^{2+}_{0.63}Fe^{3+}_{11}O_{19}$. Already at low substitution amounts FeO is incorporated in the M-type structure. Up to about 8 mol% divalent iron was detected in the crystal structure of the hexaferrite. It is remarkable that the ratio of FeO to CoO in the La-hexaferrite end member is not balanced. The amount of FeO is

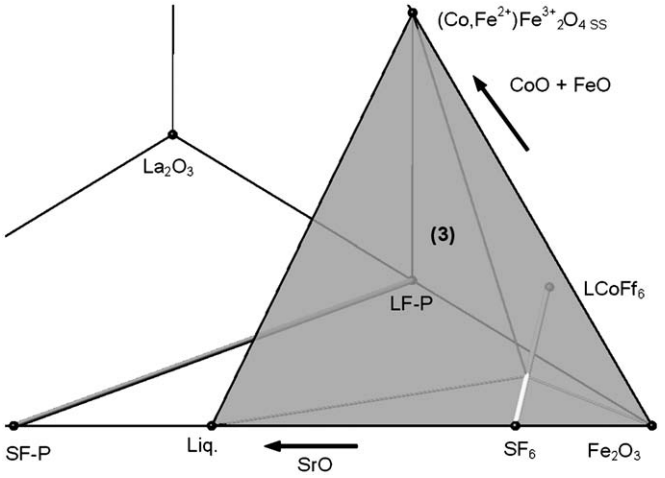

Fig. 7. Phase relations including phase polyhedron (3) La-perovskite—Co–Fe spinel$_{SS}$—M-type$_{SS}$—hematite in the Fe-rich part of the system Sr–La–Co–Fe–O at 1300 °C (bold light grey lines = solid solution series); SF–P = Sr-perovskite $SrFeO_{3-\delta}$; LF–P = La-perovskite $LaFeO_3$; $LCoFf_6$ = M-type $LaFe^{2+}_{0.6}Co_{0.4}Fe^{3+}_{11}O_{19}$; SF_6 = M-type Sr-hexaferrite $SrFe^{3+}_{12}O_{19}$; $(Co,Fe^{2+})Fe^{3+}_2O_{4\,SS}$ = spinel$_{SS}$; S = SrO; L = La_2O_3; Co = CoO; F = Fe_2O_3; f = FeO.

about 1.5 times higher than those of CoO (FeO/CoO = 1.5). The ratio FeO/CoO depends on different factors like the chemical composition of the starting mixtures and the phase assemblages. This will be discussed more in detail in Section 3.4 of this paper. The substitution formula at 1300 °C shows the complete solid solution and the larger amount of small divalent ions (Fe^{2+}, Co^{2+}) compared with 1200 °C:

$Sr_{1-x}La_xCo^{2+}{}_yFe^{2+}{}_{x-y}Fe^{3+}{}_{12-x}O^{19}$

La^{3+}: $0 \le x \le 1$

Co^{2+}: $0 \le y \le 0.40$ and Fe^{2+}: $0 \le x-y \le 0.57$

The phases which were analysed are similar to the phase assemblages at 1200 °C (Figs. 6–8). There are a solid solutions series of pervoskite $Sr_{1-x}La_xFeO_{3-\delta}$ ($0 \le \delta \le 0.5$ and $0 \le x \le 1$) and spinel$_{SS}$ $Co_{1-x}Fe^{2+}{}_xFe^{3+}{}_2O_4$ ($0 \le x \le 0.70$). In addition, similar to the system Sr–Fe–O a Sr-rich liquid phase was determined [21,22]. The composition of the melt was not measured, as already mentioned above. Therefore their composition was drawn according to the system Sr–Fe–O after Goto and Takahashi [22]. Finally hematite completes the phase assemblages.

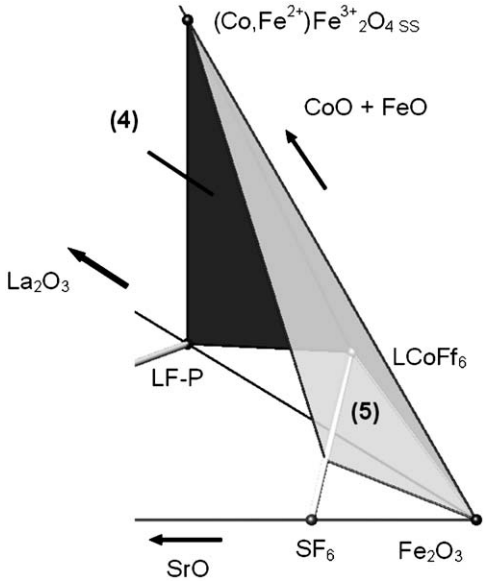

Fig. 8. Phase relations including phase polyhedra (4) liquid—Co–Fe spinel$_{SS}$—M-type$_{SS}$—hematite and (5) Co–Fe spinel$_{SS}$—M-type$_{SS}$—hematite in the Fe-rich part of the system Sr–La–Co–Fe–O at 1300 °C (bold light grey lines = solid solution series); SF–P = Sr-perovskite $SrFeO_{3-\delta}$; LF–P = La-perovskite $LaFeO_3$; $LCoFf_6$ = M-type $LaFe^{2+}_{0.6}Co_{0.4}Fe^{3+}_{11}O_{19}$; SF_6 = M-type Sr-hexaferrite $SrFe^{3+}_{12}O_{19}$; $(Co,Fe^{2+})Fe^{3+}_2O_4$ $_{SS}$ = spinel$_{SS}$; S = SrO; L = La_2O_3; Co = CoO; F = Fe_2O_3; f = FeO.

3.3. Hexaferrites and phase relations at 1380 °C

The solid solution at 1380 °C is continuous (Table 4; Fig. 9). But contrary to the solid solution at 1300 °C only on the Fe-rich side, facing magnetite (mixtures 6–9), a continuous solid solution range could be determined. A nearly Sr-free M-type could be determined. The Sr-free end member $LaCo_{0.1}Fe^{2+}_{0.9}Fe^{3+}_{11}O_{19}$ measured in the system La–Co–Fe–O was added in Table 4, but will be described in much more detail in a forthcoming paper. On the Fe-poor side (mixtures 2–4), the substitution amount is limited (maximum substitution amount found in mixture 4: ~60%). Due to the increasing temperature the amount of incorporated FeO in the M-type reaches its maximum at about 13 mol%. The referring substitution formula shows that the ratio of FeO/CoO is significantly higher than at lower temperatures (1200, 1300 °C), especially at high substitution amounts:

$Sr_{1-x}La_xCo^{2+}{}_yFe^{2+}{}_{x-y}Fe^{3+}{}_{12-x}O^{19}$

La^{3+}: $0 \le x \le 1$

Co^{2+}: $0 \le y \le 0.10$ and Fe^{2+}: $0 \le x-y \le 0.90$

As shown in Tables 3 and 4 it is not possible to predict the ratio FeO/CoO in the M-type hexaferrite with known substitution amount x (La-content). The reasons for that will be discussed in the following Section 3.4 of this paper. Despite this, the study of the phase relations reveals a second hexaferrite, the W-type ferrite ($SrFe^{2+}_2Fe^{3+}_{16}O_{27}$) which is also a hard magnetic compound (Fig. 9). This W-type contains FeO and formed a solid solution by incorporation of additional FeO, CoO and La_2O_3 similar to the M-type. Results of the microprobe measurements show the substitution principle $Sr^{2+}+Fe^{3+} \leftrightarrow La^{3+}+(Co^{2+}, Fe^{2+})$. The substitution formula demonstrates the small extent of the solid solution

Table 4
M-type and W-type hexaferrites at 1380 °C in the system Sr–La–Co–Fe–O.

M-type and W-type hexaferrites at 1380 °C								
Mixtures	SrO (mol%)	La_2O_3 (mol%)	CoO (mol%)	FeO (mol%)	Fe_2O_3 (mol%)	La^{3+} x	Co^{2+} y	Fe^{2+} $x-y$
6	11.1	1.4	0.8	2.4	84.3	0.20	0.06	0.17
2	9.0	2.6	2.9	2.4	83.1	0.36	0.20	0.17
7	8.8	2.6	1.2	4.3	83.1	0.36	0.09	0.30
3	8.0	3.1	3.1	3.2	82.6	0.44	0.22	0.22
6(W-type)*	*7.4*	*0.7*	*2.8*	*17.1*	*72.0*	*0.16*	*0.31*	*1.88**
8	6.9	3.5	2.0	5.4	82.2	0.50	0.14	0.38
4	5.9	4.3	3.0	5.4	81.4	0.60	0.21	0.38
9	1.0	1.9	1.9	11.3	79.2	0.91	0.14	0.79
*	–	7.1	1.5	12.8	78.6	1.00	0.10	0.90

M-type solid solution series: $Sr_{1-x}La_xFe^{2+}{}_{x-y}Co^{2+}{}_yFe^{3+}{}_{12-x}O^{19}$ ($0 \le x \le 1$ and $0 \le y \le 0.2$); W-type: $Sr_{1-x}La_xCo_yFe^{2+}_{2+x-y}Fe^{3+}_{16-x}O_{27}$ ($0 \le x \le 0.2$ and $0 \le y \le 0.3$); 1.88* = portion of Fe^{2+} in the W-type = $2+x-y$; * = pure La end member of the M-type$_{SS}$ observed in the La–Co–Fe–O system, derived from a forthcoming paper.

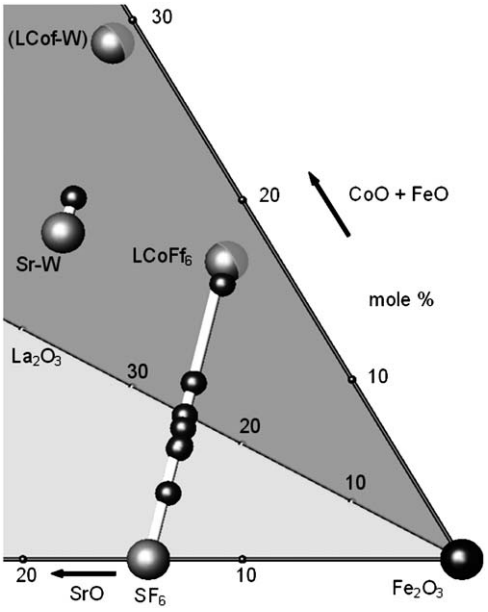

Fig. 9. M-type solid solution series $Sr_{1-x}La_xFe^{2+}{}_{x-y}Co^{2+}{}_yFe^{3+}{}_{12-x}O^{19}$ ($0 \le x \le 1$ and $0 \le y \le 0.2$) and W-type solid solution series $Sr^{2+}_{1-x}La^{3+}{}_xCo_yFe^{2+}_{2+x-y}Fe^{3+}_{16-x}O_{27}$ ($0 \le x \le 0.2$ and $0 \le y \le 0.3$) at 1380 °C; dark grey = data from electronprobe microanalyses; $SF_6 = SrFe^{3+}_{12}O_{19}$; $LCoFf_6 = LaCo_{0.1}Fe^{2+}_{0.9}Fe^{3+}_{11}O_{19}$; Sr–W = $SrFe^{2+}_2Fe_{16}O_{27}$; LCof–W = hypothetic $LaCo_yFe^{2+}_{3-y}Fe_{15}O_{27}$; S = SrO; L = La_2O_3; Co = CoO; F = Fe_2O_3; f = FeO.

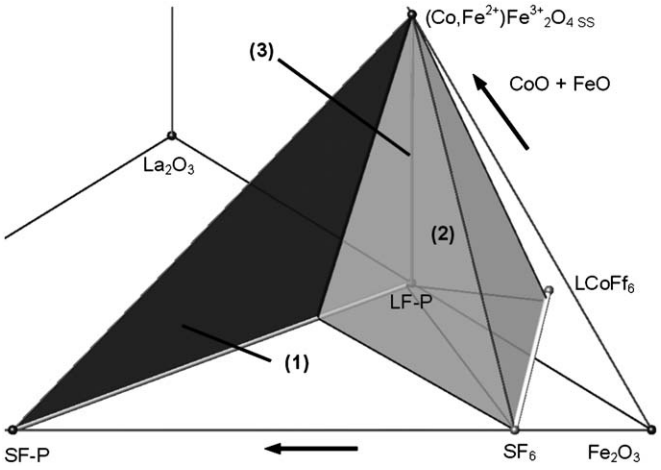

Fig. 10. Phase relations including phase polyhedra (1) perovskite$_{SS}$—Co–Fe spinel$_{SS}$, (2) perovskite$_{SS}$—M-type$_{SS}$—Co–Fe spinel$_{SS}$ and (3) La-perovskite—Co–Fe spinel$_{SS}$ in the Fe-rich part of the system Sr–La–Co–Fe–O at 1380 °C (bold light grey lines = solid solution series); SF–P = Sr-perovskite $SrFeO_{3-\delta}$; LF–P = La-perovskite $LaFeO_3$; $LCoFf_6$ = M-type $LaFe^{2+}_{0.9}Co_{0.1}Fe^{3+}_{11}O_{19}$; SF_6 = M-type Sr-hexaferrite $SrFe^{3+}_{12}O_{19}$; $(Co,Fe^{2+})Fe^{3+}_2O_{4\,SS}$ = spinel$_{SS}$; S = SrO; L = La_2O_3; Co = CoO; F = Fe_2O_3; f = FeO.

series between the end members $SrFe^{2+}_2Fe^{3+}_{16}O_{27}$ and $Sr_{0.84}La_{0.16}Co_{0.31}Fe^{2+}_{1.88}Fe^{3+}_{15.84}O_{27}$:

$$Sr_{1-x}La_xCo_yFe^{2+}_{2+x-y}Fe^{3+}_{16-x}O_{27}$$

$$La^{3+}\text{: } 0 \le x \le 0.16$$

$$Co^{2+}\text{: } 0 \le y \le 0.31 \text{ and } Fe^{2+}\text{: } 2 \ge 2+x-y \ge 1.88$$

To examine this solid solution and to check the physical properties of this hard magnetic compound further studies are required.

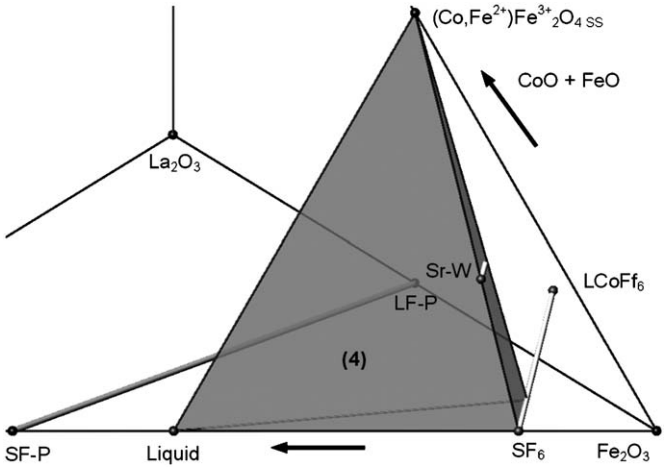

Fig. 11. Phase relations including phase polyhedron (4) liquid—M-type$_{SS}$—W-type$_{SS}$—Co–Fe spinel$_{SS}$ in the Fe-rich part of the system Sr–La–Co–Fe–O at 1380 °C (bold light grey lines = solid solution series); SF–P = Sr-perovskite $SrFeO_{3-\delta}$; LF–P = La-perovskite $LaFeO_3$; $LCoFf_6$ = M-type $LaFe^{2+}_{0.9}Co_{0.1}Fe^{3+}_{11}O_{19}$; SF_6 = M-type Sr-hexaferrite $SrFe^{3+}_{12}O_{19}$; $(Co,Fe^{2+})Fe^{3+}_2O_{4\,SS}$ = spinel$_{SS}$; Sr-W: Sr end member of the solid solution series $Sr_{1-x}La_xCo_yFe^{2+}_{2+x-y}Fe^{3+}_{16-x}O_{27}$ ($0 \le x \le 0.2$) ($0 \le y \le 0.3$), S = SrO; L = La_2O_3; Co = CoO; F = Fe_2O_3; f = FeO.

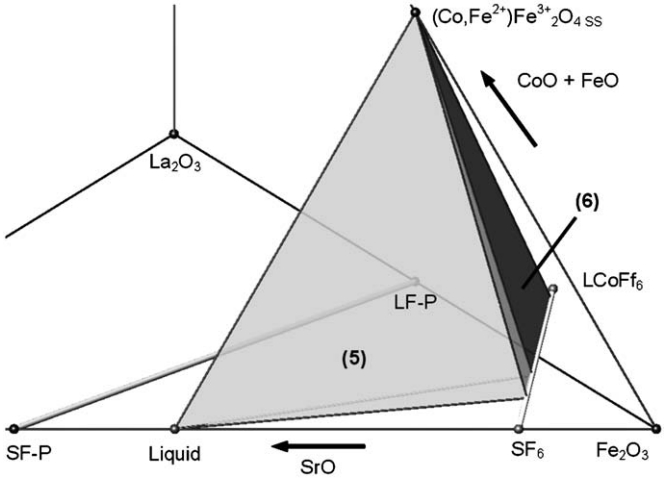

Fig. 12. Phase relations including phase polyhedra (5) liquid—M-type$_{SS}$—Co–Fe spinel$_{SS}$ and (6) M-type$_{SS}$—Co–Fe spinel$_{SS}$ in the Fe-rich part of the system Sr–La–Co–Fe–O at 1380 °C (bold light grey lines = solid solution series); SF–P = Sr-perovskite $SrFeO_{3-\delta}$; LF–P = La-perovskite $LaFeO_3$; $LCoFf_6$ = M-type $LaFe^{2+}_{0.9}Co_{0.1}Fe^{3+}_{11}O_{19}$; SF_6 = M-type Sr-hexaferrite $SrFe^{3+}_{12}O_{19}$; $(CoFe^{2+})Fe^{3+}_2O_{4\,SS}$ = spinel$_{SS}$; S = SrO; L = La_2O_3; Co = CoO; F = Fe_2O_3; f = FeO.

Nevertheless the coexisting phases are similar to these found at lower temperatures (Figs. 10–12). The FeO content in the Co–Fe spinel$_{SS}$ increases up to 50 mol% in the magnetite $Fe^{2+}Fe^{3+}_2O_4$, according to the phase diagram Fe–Co–O [20]. In addition to the spinel$_{SS}$ $Co_{1-x}Fe^{2+}{}_xFe^{3+}{}_2O_4$ ($0 \le x \le 1$) a complete solid solution of the Sr/La–Fe perovskite $Sr_{1-x}La_xFeO_{3-\delta}$ ($0 \le \delta \le 0.5$ and $0 \le x \le 1$) was observed.

3.4. The higher-dimensional solid solution range of M-type hexaferrites—reasons for the varying ratio CoO/FeO

A higher dimension of the most striking solid solution mechanism $Sr^{2+}+Fe^{3+} \leftrightarrow La^{3+}+(Co^{2+}, Fe^{2+})$ could be observed. The amounts of Co^{2+} and Fe^{2+} in the M-type hexaferrite vary with the chemical composition of the starting mixtures (Fig. 13a–c) at all examined temperatures. At 1300 and 1380 °C higher amounts

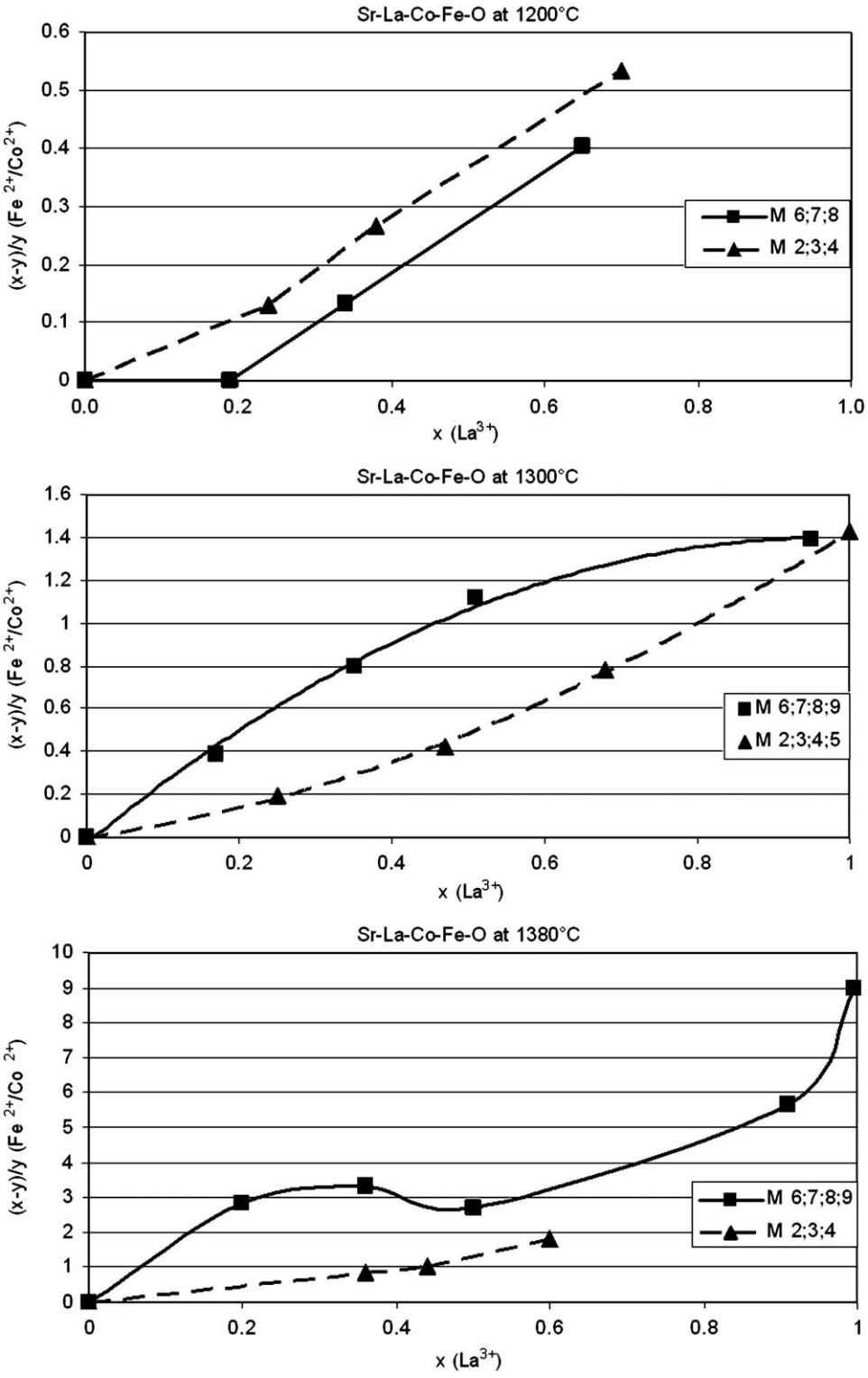

Fig. 13. (a)–(c) Fe^{2+}/Co^{2+} $(x-y/y)$ in dependence on the substitution grade La^{3+} (x) of the M-type $Sr_{1-x}La_xCo_y{}^{2+}Fe^{2+}{}_{x-y}Fe^{3+}_{12-x}O_{19}$ at 1200 (a); 1300 (b) and 1380 °C (c); M 6–8 = Mixtures 6–8 which contain a significant higher amount Fe_2O_3 than mixtures 2–4 (M 2–4).

of Fe_2O_3 in starting mixtures cause higher FeO contents in the formed M-types (Fig. 13b and c). In Table 4 one should compare mixtures 2 and 7. Regardless of the same substitution amounts, the two M-types differ in FeO and CoO contents. Therefore with a known substitution of x (La_2O_3 content) it is not possible to predict the ratio CoO/FeO. Besides that, the coexisting phases influence the amount of incorporated ions. At 1200 °C only in the Fe-rich region (mixtures 6–9) $Fe^{2+}O$ bearing Co–Fe spinel is detectable. This $spinel_{SS}$ ($Co_{1-x}Fe^{2+}{}_xFe^{3+}{}_2O_4$ $(0 \leq x \leq 0.45)$) competes with the M-type for the Fe^{2+}-ions. Therefore the M-type hexaferrites in the mixtures with lower amounts of iron (mixtures 2–5) contain more FeO, because of the absence of Co–Fe $spinel_{SS}$ in the phase assemblages (Fig. 13a). At 1300 and 1380 °C in all samples a Co–Fe $spinel_{SS}$ was detected. Hence in the Fe-rich

mixtures also the FeO-rich M-type hexaferrite is formed (Fig. 13b and c). Finally it should be mentioned that with rising temperatures the amount of FeO in the M-types also increases. The aim of further studies should be the investigation of the higher dimensional substitution mechanisms in much more detail.

4. Conclusions

The M-type hexaferrites and their substitution mechanism in the system Sr–La–Co–Fe–O were examined in air. At 1200, 1300 and 1380 °C extensive solid solution ranges were observed. Divalent iron is always incorporated in the crystal structure. The resulting substitution principle $Sr^{2+}+Fe^{3+} \leftrightarrow La^{3+}+(Co^{2+}, Fe^{2+})$ yields to a higher dimensional range of the solid solution because of the different amounts of the incorporation of CoO and FeO. CoO occupies the majority of the small cation positions in the M-type structure at 1200 °C, rarely exclusive at low substitution amounts ($<25\%$). However at 1300 °C the Fe^{2+}-ions predominate and at 1380 °C considerably higher amounts of Fe^{2+}-ions were observed in the M-type structure (1200 °C: $Fe^{2+}_{max}/Co^{2+}_{max}$~0.5; 1300 °C: $Fe^{2+}_{max}/Co^{2+}_{max}$~1.5; 1380 °C: $Fe^{2+}_{max}/Co^{2+}_{max}$~4.5). Amounts up to 11 mol% FeO are incorporated in the hexaferrite crystal lattice at 1380 °C. It was proved that the solid solution series of M-type hexaferrite is not a simple one-dimensional mechanism. The ratio FeO/CoO and therefore the extent of the higher dimensional range of the solid solutions depend on the temperature, the phase assemblages and the chemical composition of the starting mixtures (supply of FeO_x). The results of this work should help to understand the behaviour of magnetic materials and to calculate magnetic properties.

Acknowledgments

The authors are grateful for the titrations experiment that were accomplished by Mrs. Daniela Seifert (F.H. Jena). This work was supported by a grant (GO-606/7-3) from the Deutsche Forschungsgemeinschaft (DFG), Germany.

References

[1] W. Hart, in: Proceedings of the Conference Iron Oxides for Hard/Soft Ferrites, Gorham-Intertec, Pittsburgh, 1996.
[2] B.T. Shirk, W.R. Bussem, J. Appl. Phys. 10 (1969) 1294–1296.
[3] J. Töpfer, S. Schwarzer, S. Senz, D. Hesse, J. Eur. Ceram. Soc. 25 (2005) 1681–1688.
[4] J. Smith, H.P.J. Wijn, Ferrites, Philips' Technical Library, 1959.
[5] H. Stablein, in: E.P. Wohlfarth (Ed.), Ferromagnetic Materials, vol. 3, North-Holland, Amsterdam, 1982.
[6] A. Wesselsky, Diploma Thesis, Institute of Geology and Mineralogy, Department of Applied Mineralogy, Friedrich-Alexander-University of Erlangen-Nuremberg, 2003, 113pp.
[7] A. Wesselsky, M. Göbbels, S. Schwarzer, J. Töpfer, in: Ninth International Conference Ferrites, ICF-9, 2004, pp. 45–50.
[8] Y. Ogata, Y. Kubota, T. Takami, M. Tokunaga, T. Shinohara, IEEE Trans. Magn. 35 (5) (1999) 3334–3336.
[9] K. Iida, Y. Minachi, K. Masuzarawa, M. Kawakami, H. Nishio, H. Taguchi, J. Magn. Soc. Jpn. 23 (4–2) (1999) 1093–1096.
[10] H. Taguchi, Y. Minachi, K. Masuzawa, H. Nishio, in: Proceedings of Eighth International Conference Ferrites, Kyoto, Tokyo, 2000, pp. 405–409.
[11] Y. Kubota, T. Takami, Y. Ogata, in: Proceedings of Eighth International Conference Ferrites, Kyoto, Tokyo, 2000, pp. 410–412.
[12] A. Morel, F. Kools, P. Tenaud, R. Grössinger, M. Rossignol, Jpn. Soc. Pwd. Pwd. Metall.;
A. Morel, F. Kools, P. Tenaud, R. Grössinger, M. Rossignol, in: Eighth International Conference Ferrites (ICF-8), Kyoto, Tokyo, 2000, pp. 434–436.
[13] G. Wiesinger, M. Müller, R. Grössinger, M. Pieper, A. Morel, F. Kools, P. Tenaud, J.M. Le Breton, J. Kreisel, Phys. Stat. Sol. (a) 189 (2) (2002) 499–508.
[14] L. Lechevallier, J.M. Le Breton, J. Teillet, A. Morel, F. Kools, P. Tenaud, Physica B 327 (2003) 135–139.
[15] D. Ravinder, P. Shalini, P. Mahesh, A. Morel, P. Tenaud, J. Alloys Compd. 363 (2004) 68–74.
[16] P. Tenaud, A. Morel, F. Kools, J.F. Le Breton, L. Lechevallier, J. Alloys Compd. 370 (2004) 331–334.
[17] A. Richter, Private Communication, Department of Applied Mineralogy, University of Erlangen-Nuremberg, 2006.
[18] M. Okrusch, S. Matthes, Springer, 7. Auflage, Berlin, 2005, p. 477.
[19] N. Langhof, D. Seifert, M. Göbbels, J. Töpfer, J. Solid State Chem. (2009), submitted for publication.
[20] D.P. Masse, A. Muan, J. Am. Ceram. Soc. 48 (9) (1965) 466–469.
[21] P. Batti, Ann. Chim. (Rome) 52 (9–10) (1962) 941–961.
[22] Y. Goto, K. Takahashi, J. Jpn. Soc. Pwd. Pwd. Metall. 17 (1971) 193–197.